

MAGNETIC AND MICROWAVE ABSORBING PROPERTIES IN SEMI-HARD $\text{Co}_x\text{Fe}_{(3-x)}\text{O}_4$ SYNTHESIZED BY SOL-GEL METHOD

Akmal Johan^{a*}, Dedi Setiabudidaya^a, Fitri Suryani Arsyad^a, Mashadi^b, Yosef Sarwanto^b, Didin Sahidin Winatapura^b, Yana Taryana^c, Yunasfi^b, Wisnu Ari Adi^{b*}

Article history

Received
30 September 2021
Received in revised form
16 May 2023
Accepted
11 June 2023
Published Online
25 June 2023

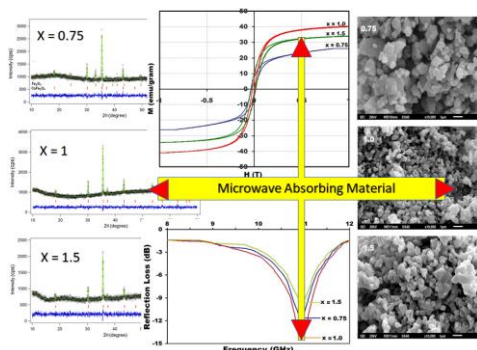
^aDepartment of Physics, Faculty of Mathematics and Natural Science, Sriwijaya University, Palembang, South Sumatra, Indonesia

^bResearch Center for Advanced Materials, National Research and Innovation Agency, Kawasan KST BJ Habibie Serpong, Tangerang Selatan, Banten, Indonesia

^cResearch Center for Telecommunication- National Research and Innovation Agency, Jl. Sangkuriang, Bandung, West Java, Indonesia

*Corresponding author
akmal_johan@mipa.unsri.ac.id

Graphical abstract



Abstract

Magnetic and microwave absorption properties of $\text{Co}_x\text{Fe}_{(3-x)}\text{O}_4$ semi-hard materials ($x = 0.75, 1.0, \text{ and } 1.5$) synthesized have been carried out using the chemical method of sol-gel. The mixture of iron nitrate $\text{Fe}_2(\text{NO}_3)_3$ and cobalt nitrate $\text{Co}(\text{NO}_3)_2$ dissolved in ethylene glycol, then the mixture was heated while stirring at 60°C for 1 hour to form a gel. After that dried at a temperature of 120°C for 5 hours. A fine powder of $\text{Co}_x\text{Fe}_{(3-x)}\text{O}_4$ was obtained through the grinding process. The $\text{Co}_x\text{Fe}_{(3-x)}\text{O}_4$ powder crystallization was done by sintering at 1000°C for 5 hours. The X-Ray Diffraction (XRD), Scanning Electron Microscope (SEM), Vibrating-sample magnetometer (VSM), and Vector Network Analyzer (VNA) is used to investigate phase identification, particle morphology, magnetic properties, and microwave absorption ability, respectively. Based on the phase identification show that the samples with composition $x = 0.75$ have two phases, namely CoFe_2O_4 and Fe_2O_3 . The sample composition for $x \geq 1$ is a single phase of CoFe_2O_4 . The particle morphology is homogeneous with spherical and the particle size is about $100 - 500$ nm. The samples act ferromagnetic behavior with a saturation magnetization (M_s) of $26.1-40.4$ emu/g and coercivity field (H_c) of $223-299$ Oe. The maximum reflection loss (RL) value of -14.03 dB at the frequency 10.98 GHz occurred in a single-phase sample with a composition of $x = 1.0$. This study provided a new composite material with great potential for the development of microwave-absorbing materials.

Keywords: Magnetic materials, $\text{Co}_x\text{Fe}_{(3-x)}\text{O}_4$ system, sol-gel method, magnetic properties, microwave absorption, reflection loss

© 2023 Penerbit UTM Press. All rights reserved

1.0 INTRODUCTION

Research on microwave-absorbent materials has become extremely important because of the rapid

development of technology in electronics and telecommunications for microwave protection and anechoic chambers. Microwave-absorbing materials as protection are used to overcome

α electromagnetic wave interference because they can absorb and eliminate the energy emitted by the microwave source [1, 2]. Much effort is to find the ideal microwave-absorbing material to increase microwave absorption. Starting from research on the material itself to its geometric design. Generally, ideal microwave-absorbing materials have several characteristics of light, broadband, thin, and resistance to heat and chemistry change [2, 3].

Microwave absorbent materials that are relatively cheap and abundant are ferrite-based magnetic materials. There are many types of ferrite-based materials, namely M, W, Y, X, and Z types and spinel ferrite types. Spinel ferrite is more stable compared to other types because it has a simple structure and a high resistivity. It is also a potential material candidate for microwave absorbers in a wide frequency range from C-band (5.85-8.20 GHz) to X-band (8.20-12.4 GHz) frequencies [4]. The main characteristic of microwave-absorption materials has to have a value of permeability and permittivity and behaves as a semi-hard magnet. Spinel ferrite material that has these characteristics is cobalt ferrite [5, 6]. Cobalt ferrite with the chemical formula CoFe_2O_4 shows a fully reverse spinel structure with ferromagnetic behaviour below 790 K. The magnetic interaction of this cobalt ferrite structure is very strong. CoFe_2O_4 is dominated by inverted oxide spinels with Co^{2+} ions at site B and Fe^{3+} ions evenly distributed at sites A and B [7, 8]. In addition, this material has a high Curie temperature, moderate anisotropy magnetocrystalline, high magnetostrictive coefficient, and is chemically stable [9, 10]. Therefore, the CoFe_2O_4 material has the potential for applications as a microwave absorber [8, 11].

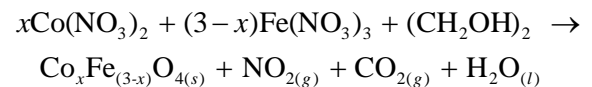
It is known that ferrite spinel structures are of three types, namely normal, inverted, and mixed ferrite, depending on the position of the divalent and trivalent metal ions. A normal ferrite in which all the tetrahedral sites (A) are occupied by eight divalent cations and the octahedral sites (B) by 16 trivalent metal ions $[\text{A}^{2+}\text{B}^{3+}_2]\text{O}^{2-}_4$. An inverted ferrite in which eight of the 16 trivalent metal ions occupy the tetrahedral sites, and the octahedral sites are occupied by eight divalent metal ions and eight trivalent cations $[\text{B}^{3+}][\text{A}^{2+}\text{B}^{3+}_1]\text{O}^{2-}_4$. Meanwhile, mixed ferrites where the tetrahedral and octahedral sites are occupied randomly by divalent and trivalent metal ions $[\text{A}^{2+}_x\text{B}^{3+}_{1-x}][\text{A}^{2+}_{1-x}\text{B}^{3+}_{1+x}]\text{O}^{2-}_4$. As a microwave absorbing material, the material must have high complex permeability and permittivity in a single phase so that it is expected to provide an opportunity to have magnetic properties and high dielectric losses.

In previous studies, CoFe_2O_4 material has been prepared and reported through chemical and physical processes [4, 7-8, 10]. However, from some of the literature there has not been found research that integrates the selection of the right type of spinel ferrite for use as a microwave absorbent material. In addition, this study chose the sol-gel method to obtain CoFe_2O_4 nanoparticles because this method

is known as one of the most promising processes for obtaining nano-sized materials. The chemical formula in this study is $\text{Co}_x\text{Fe}_{(3-x)}\text{O}_4$ with ($x = 0.75, 1.0$ and 1.5). These three compositions are expected to be able to represent the three types of spinel ferrite, namely inverse, normal, and mixed ferrite successively. Thus this research aims to make semi-hard magnets based on $\text{Co}_x\text{Fe}_{(3-x)}\text{O}_4$ and it is hoped that the most appropriate composition can be obtained as a material that has the best microwave absorption ability.

2.0 METHODOLOGY

Iron Nitrate ($\text{Fe}(\text{NO}_3)_3 \cdot 9\text{H}_2\text{O}$) (Merck), Cobalt Nitrate ($\text{Co}(\text{NO}_3)_2 \cdot 6\text{H}_2\text{O}$) (Merck) was mixed and dissolved in ethylene glycol with chemical formula reaction as follows :



The sample was heated and stirred at 60°C for 1 hour to gel. After that, it was dried at 120°C for 5 hours and pulverized to obtain $\text{Co}_x\text{Fe}_{(3-x)}\text{O}_4$ fine powder with ($x = 0.75, 1.0$ and 1.5). The sample was sintered at 1000°C . for 5 hours in the end process.

Phase identification of the sample was carried out by using X-ray Diffraction (XRD) of PW1710 Empyrean Panalytical type with radiation $\text{CuK}\alpha$ ($\lambda = 1.5406 \text{ \AA}$) at range angle of $10^\circ - 80^\circ$ and step size of 0.02° . The particle morphology was observed by SEM (Scanning Electron Microscope) of JEOL, JSM-6510 LA type. Meanwhile, the magnetic properties of the samples were obtained from VSM (Vibrating Sample Magnetometer) of OXFORD type at magnetic range -1 up to 1 Tesla. The last characterization is the ability of microwave absorption by using VNA (Vector Network Analyzer) of Advatest-R3370 type in the range 8 GHz - 12 GHz (X-Band).

3.0 RESULTS AND DISCUSSION

The diffraction spectra in the range $10^\circ - 70^\circ$ for various compositions x of $\text{Co}_x\text{Fe}_{(3-x)}\text{O}_4$ system ($x = 0.75, 1.0,$ and 1.5) are denoted in Figure 1. The formed diffraction pattern shows that the composition with value $x = 0.75$ was formed with two phases, namely Fe_2O_3 and CoFe_2O_4 phases. On the other hand, compositions with values $x \geq 1$ indicate that the sample is a single phase of CoFe_2O_4 .

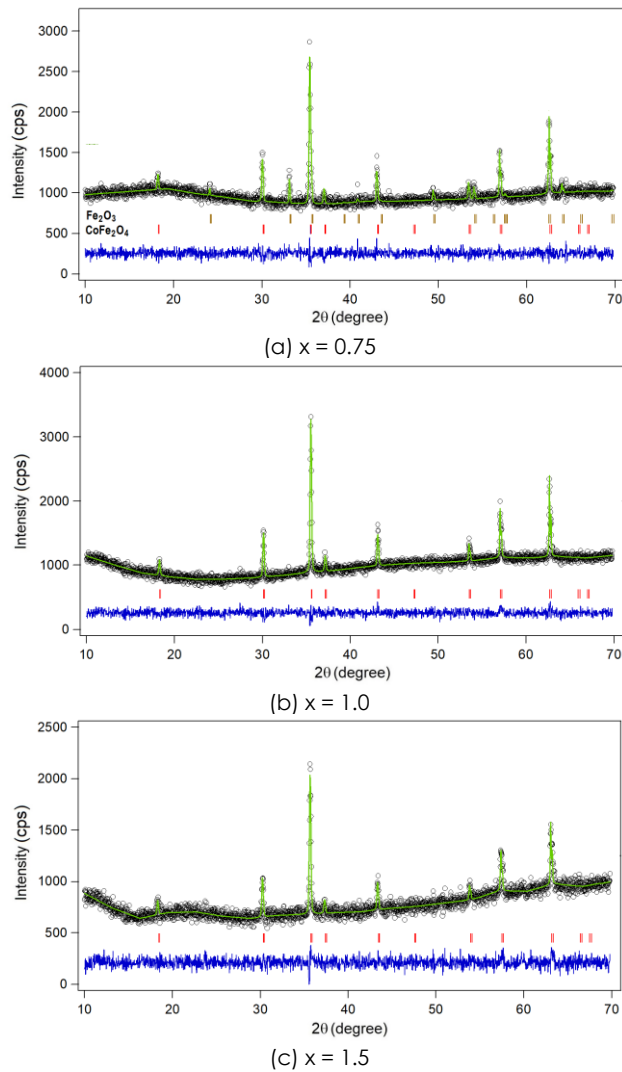


Figure 1 Refinement result of XRD pattern of the $\text{Co}_x\text{Fe}_{(3-x)}\text{O}_4$ system with ($x=0.75$; 1.0 dan 1.5)

The Fe_2O_3 phase has a hexagonal crystal structure with the highest peak of the (104) crystallographic plane (104) appearing at an angle of 33° and another peak characteristic of Fe_2O_3 at an angle of 24° , 36° , 41° , 54° , 63° , and 66° are the crystal planes (012), (110), (113), (024), (300), and (125), respectively, corresponding to ICDD database 96-901-5965. On the other hand, the CoFe_2O_4 phase has a main peak at an angle of about 35° , which is the highest peak of the crystal plane (311). CoFe_2O_4 has a cubic structure with space group $\text{Fd}3\text{m}$. This analysis reveals a second peak that is also characteristic of CoFe_2O_4 : crystallographic plane peaks (111), (220), (222), (400), (511), (422), and (440). Enhanced by presence at angles of approximately 18° , 30° , 37° , 43° , 53° , 57° , and 64° , respectively. This phase identification is related to that of Xavier's report in 2014 [12] and the ICDD database 96-100-6117.

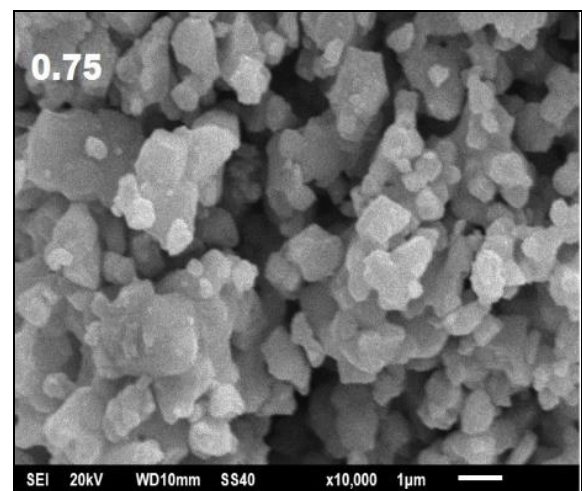
Further analysis of the XRD pattern of the $\text{Co}_x\text{Fe}_{(3-x)}\text{O}_4$ for $x = 0.75$, 1.0, and 1.5 system material was carried out using the GSAS program which was

calculated based on the XRD pattern refinement results. General structure analysis system (GSAS) is a crystallographic modelling software obtained based on the analysis of the XRD pattern structure [13]. In this study it was used to analyse the XRD pattern of $\text{Co}_x\text{Fe}_{(3-x)}\text{O}_4$ samples. This GSAS software is very comprehensive and is expected to be able to explain the complexity of the $\text{Co}_x\text{Fe}_{(3-x)}\text{O}_4$ structure. Statistical parameters to measure the degree of suitability of the Bragg diffraction pattern between the experimental result profile and the calculated result profile based on input from the database are χ^2 (goodness of fit) and R_{wp} (weighted profile residual) as shown in Figure 1. The results of this refinement show that the observation and calculation curve resulted in a good fitting, as shown in Table 1.

Table 1 Detailed refinement results for all variation of $\text{Co}_x\text{Fe}_{(3-x)}\text{O}_4$ system with ($x = 0.75$, 1.0, and 1.5)

Sample	$x = 0.75$	$x = 1.0$	$x = 1.5$
Phase	CoFe_2O_4	Fe_2O_3	CoFe_2O_4
Crystal structure	Cubic	Hexagonal	Cubic
Lattice parameter (Å)	$a=b=c=8.381$	$a=b=5.028$ $c=13.735$	$a=b=c=8.374$
Volume (Å ³)	588.596	300.781	576.026
ρ (gr.cm ⁻³)	9.080	5.290	5.014
χ^2	1.318	1.273	1.292

The surface morphology observations of the $\text{Co}_x\text{Fe}_{(3-x)}\text{O}_4$ sample ($x = 0.75$, 1.0 and 1.5) by using a scanning electron microscope (SEM) at 10,000x magnification are shown in Figure 2.



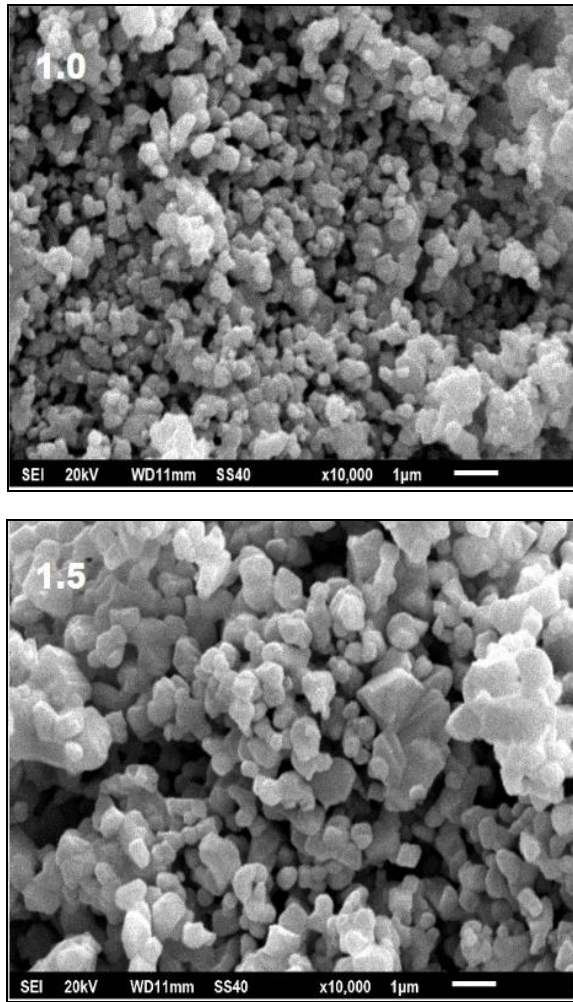


Figure 2 SEM image of the $\text{Co}_x\text{Fe}_{(3-x)}\text{O}_4$ system with ($x = 0.75; 1.0$ and 1.5)

The $\text{Co}_x\text{Fe}_{(3-x)}\text{O}_4$ samples exhibit homogeneous and evenly distributed particles across the sample surface, and the particles are composed of fine particles of varying sizes and shapes. Particle sizes range from 100 nm to 500 nm and consist of multiple large and small particles. For the value $x = 0.75$, the sample appears to consist of two different mean particle sizes. On the other hand, values of $x \geq 1.0$ have a uniform grain size. These are consistent with the XRD results showing that sample values at $x = 0.75$ contain two phases and values at $x \geq 1.0$ is single phase.

The magnetic properties of the $\text{Co}_x\text{Fe}_{(3-x)}\text{O}_4$ ($x = 0.75, 1.0$, and 1.5) system synthesized by the sol-gel method were characterized using VSM. The results of this characterization are represented by M-H hysteresis curves in the magnetic field range -1 Tesla to 1 Tesla. This curve provides information on the magnitude of the remanent magnetization (M_r), saturation magnetization (M_s), and coercivity field (H_c) as shown in Figure 3. The results of observation show that all samples as ferromagnetic behavior with moderate coercivity values (semi-hard). The detailed

values of the magnetic parameters for each sample from the hysteresis curve are displayed in Table 2.

Table 2 Magnetic properties of the $\text{Co}_x\text{Fe}_{(3-x)}\text{O}_4$ system with ($x = 0.75; 1.0$ and 1.5)

x	Sample	M_s (emu/g)	M_r (emu/g)	H_c (Oe)
0.75	$\text{Co}_{0.75}\text{Fe}_{2.25}\text{O}_4$	26.1	7.2	296
1.0	CoFe_2O_4	40.4	11.6	223
1.5	$\text{Co}_{1.5}\text{Fe}_{1.5}\text{O}_4$	34.1	10.5	299

An increase in x concentration can be interpreted as an addition to the CO_2 content in the sample. The conditions affect the value of M_s increases and the change in H_c value is not linear. The lowest magnetization value occurs at the composition $x = 0.75$ and is associated with the phase analysis where the sample has two phases, namely the phases of CoFe_2O_4 and Fe_2O_3 . It means that the M_s value depends on the mass fraction of CoFe_2O_4 . Meanwhile, the Fe_2O_3 phase can increase the anisotropic energy so that it is not easy to be magnetized by an external field and the H_c value tends to become wider when it is demagnetized.

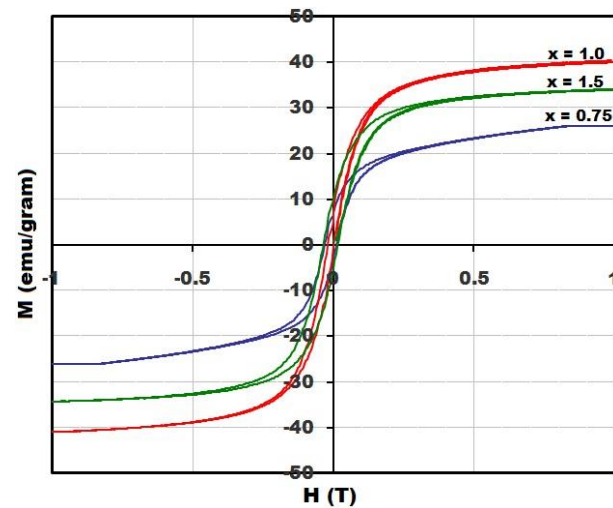


Figure 3 Hysteresis curve of the $\text{Co}_x\text{Fe}_{(3-x)}\text{O}_4$ system with ($x = 0.75, 1.0$ and 1.5)

The single phase of the sample is formed at composition $x \geq 1.0$. The sample has the highest M_s and lowest H_c values at $x = 1.0$. That is 40.4 emu/g and 223 Oe, respectively. This indicates that the total magnetic dipole moment of the material increases with ascending Co^{2+} ion content. This result is almost the same as the report of Imam *et al.* in 2014 and Nagasa *et al.* in 2015 [14], [15]. M_s is the total number of magnetic dipole moments of atoms that can be aligned in crystals per unit volume, and one factor that influences is the effective magneton number p in units of μ_B , where Co^{2+} and Fe^{3+} have p values of 6.63 and 5.92 μ_B , respectively. However, besides

increasing this p -factor value, M_s is also influenced by magnetic interactions in ferrites. The magnetic moment of ferrite is the number of magnetic moments of each sublattice [2]. The exchange interactions between the ions in this sublattice has various values. The interaction between the magnetic ions from the Co^{2+} and Fe^{3+} sublattice is the strongest compared to the Co^{2+} - Co^{2+} interactions which are almost ten times weaker, and the weakest interactions are the Fe^{3+} - Fe^{3+} interactions. At value $x = 1$ having dominant Co^{2+} - Fe^{3+} interactions lead to complete ferrimagnetism.

The last characteristic is microwave absorption ability which is presented by reflection loss (RL). The RL parameters are measured by VNA at a frequency range of 8 GHz - 12 GHz (X-Band). RL indicates the existence of a magnetic spin resonance mechanism between electromagnetic waves and materials so that microwaves are absorbed [16]. RL can be also calculated by the Equation [17]:

$$Z_{in} = \sqrt{\frac{\mu_r}{\epsilon_r}} \tanh \left[j \left(\frac{2\pi f d}{c} \right) \sqrt{\mu_r \epsilon_r} \right] \quad (1)$$

$$|\Gamma| = \frac{Z_{in} - Z_o}{Z_{in} + Z_o} \quad (2)$$

$$RL(\text{dB}) = 20 \log |\Gamma| \quad (3)$$

Where Z_{in} , Z_o , and $|\Gamma|$ are the input impedance of material, impedance free space, and reflection coefficient, respectively.

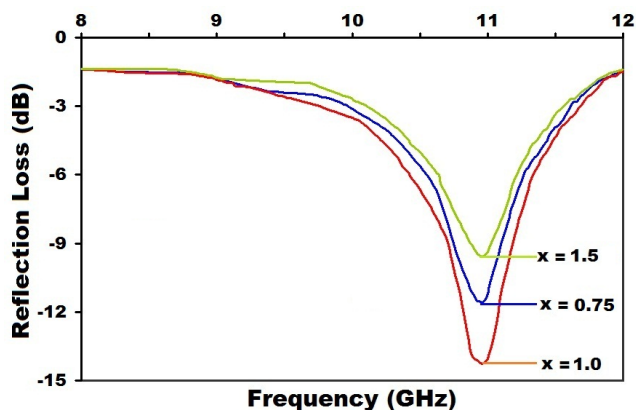


Figure 4 Reflection loss curva of the $\text{Co}_x\text{Fe}_{(3-x)}\text{O}_4$ system with ($x = 0.75$; 1.0 and 1.5)

Figure 4 shows RL curves for different concentrations x of the samples. Table 3 shows the relationship between reflection loss (RL) and microwave absorption grade obtained from VSWR Conversion Table by Marki Microwave [18]. The Microwave absorption begins to occur in the frequencies range 8 GHz to 12 GHz and peak absorption occurs at frequencies 10.98 GHz and 11 GHz. The best performance of microwave absorption

occurs on a single phase sample at $x = 1.0$ because this sample has the highest M_s and lowest H_c .

Table 3 Microwave absorption of the $\text{Co}_x\text{Fe}_{(3-x)}\text{O}_4$

x	Frequency (GHz)	RL (dB)	Absorption (%)
0.75	10.98	- 11.50	92,88
1.0	10.98	- 14.21	96,19
1.5	11.0	- 9.41	88,47

Table 3 shows that for the $\text{Co}_x\text{Fe}_{(3-x)}\text{O}_4$ system sample, the best RL values were obtained at the composition $x = 1.0$, while for $x = 0.75$ and 1.5 , the RL values decreased. This means that the composition of the $\text{Co}_x\text{Fe}_{(3-x)}\text{O}_4$ system sample affects the magnetic properties and absorption of microwaves. For compositions $x = 0.75$ and 1.5 both magnetic properties and microwave absorption decrease. According to the results of the XRD pattern analysis, it was identified that the sample with a concentration of $x = 0.75$ was identified as consisting of two phases, namely the CoFe_2O_4 and Fe_2O_3 phases, so that the magnetic properties and microwave absorption were presumably determined only by the CoFe_2O_4 phase fraction. These results are suitable with the results of research conducted by Huang, *et al.*, 2014 [19]. The greatest absorption of microwaves is shown by samples with a value of $x = 1.0$ (CoFe_2O_4 sample), which is 96.19% at 10.98 GHz. For this reason the composition of the value $x = 1.0$ is the most stable composition in the $\text{Co}_x\text{Fe}_{(3-x)}\text{O}_4$ system. Whereas for samples with a composition value of $x = 1.5$ also formed a single phase CoFe_2O_4 , but the magnetic properties and absorption of microwaves are still lower than the composition of $x = 1$ because it is suspected that the magnetic interaction of Co^{2+} - Fe^{3+} is also low. The results obtained in this study have similarities with the results of other studies although the results are still lower than those reported by Li, *et al.*, 2014 [20] and Ismail, *et al.*, 2018 [21] respective RL values of -18 dB and -28 dB.

4.0 CONCLUSION

According to this study result, it can be concluded that the synthesis of the $\text{Co}_x\text{Fe}_{(3-x)}\text{O}_4$ system ($x = 0.75$, 1.0 and 1.5) has been successfully carried out by the sol-gel method. The results of the phase analysis showed that the $\text{Co}_x\text{Fe}_{(3-x)}\text{O}_4$ sample with composition of $x < 0.75$ formed CoFe_2O_4 and Fe_2O_3 phases, while for the composition of the composition of $x \geq 1.0$ formed a single phase of CoFe_2O_4 . The measurement results of the magnetic properties of the $\text{Co}_x\text{Fe}_{(3-x)}\text{O}_4$ sample with composition of $x = 1.0$ (CoFe_2O_4 sample) showed the highest M_s value of 40.4 emu/g and the best microwave absorption, which was 96% at 10.96 GHz. Thus, composition is the main factor influencing magnetic properties and absorption of microwaves in $\text{Co}_x\text{Fe}_{(3-x)}\text{O}_4$ system

samples, where composition $x = 1$ is the best composition to obtain the best magnetic properties and microwave absorption, while for composition $x < 1.0$ or $x > 1.0$ causes the magnetic properties and absorption of microwaves to decrease. Thus, for further development as a microwave absorbing material, the CoFe_2O_4 composition which has the best magnetic properties and microwave absorption of the ferrite spinel type can be used.

Acknowledgement

The author would like to thank the Research Center for Advanced Material and Home Program of Advanced Material, National Research and Innovation Agency (BRIN), Indonesia, which provides conducting research. We gratefully acknowledge the support of the Microwave Lab of the Research Center for Telecommunication, National Research and Innovation Agency (BRIN), Indonesia for facilities research.

References

- [1] Bayrakdar, H. 2012. Electromagnetic Propagation and Absorbing Property of Ferrite-Polymer Nanocomposite Structure. *Progress in Electromagnetics Research*. 25: 269-281. <https://doi.org/10.2528/piem12072303>.
- [2] Hapishah, A. N., Syazwan, M. M., Hamidon, M. N. 2018. Synthesis and Characterization of Magnetic and Microwave Absorbing Properties in Polycrystalline Cobalt Zinc Ferrite ($\text{Co}_{0.5}\text{Zn}_{0.5}\text{Fe}_2\text{O}_4$) Composite. *Journal of Materials Science: Materials in Electronics*. 29: 20573-20579. <https://doi.org/10.1007/s10854-018-0192-9>.
- [3] Jiang, Q., Li, H., Cao, Z., Li, H., Wang, Q., Jiang, Z., Kuang, Q., Xie, Z. 2017. Synthesis and Enhanced Electromagnetic Wave Absorption Performance of Amorphous $\text{Co}_x\text{Fe}_{10-x}$ Alloys. *Journal of Alloys and Compounds*. 726: 1255-1261. <http://dx.doi.org/10.1016/j.jallcom.2017.08.066>.
- [4] Husain, M., Misbah-ul-Islam, Meydan, T., Cuenca, J. A., Melikhov, Y., Mustafa, G., Murtaza, G., Jamil, Y. 2018. Microwave Absorption Properties of CoGd Substituted ZnFe_2O_4 Ferrites Synthesized by Co-precipitation Technique. *Ceramics International*. 44(6): 5909-5914. <https://doi.org/10.1016/j.ceramint.2017.12.145>.
- [5] Jian, G., Fu, Q., Zhou D. 2012. Particles Size Effects of Single Domain CoFe_2O_4 on Suspensions Stability. *Journal of Magnetism and Magnetic Materials*. 324: 671-676. <https://doi.org/10.1016/j.jmmm.2011.08.036>.
- [6] Ding, Y., Liao, Q., Liu, S., Guo, H., Sun, Y., Zhang G., & Zhang, Y. 2016. Reduced Graphene Oxide Functionalized with Cobalt Ferrite Nanocomposites for Enhanced Efficient and Lightweight Electromagnetic Wave Absorption. *Scientific Reports* 6: 32381. <https://doi.org/10.1038/srep32381>.
- [7] Kuruva, P., Matteppanavar, S., Srinath, S. and Thomas, T. 2014. Size Control and Magnetic Property Trends in Cobalt Ferrite Nanoparticles Synthesized Using an Aqueous Chemical Route. *IEEE Transactions on Magnetics*. 50(1): 5200108. <https://doi.org/10.1109/tmag.2013.2283467>.
- [8] Ristic, M., Krehula, S., Reissner, M., Jean, M., Hannover, B., Musi, S. 2017. Synthesis and Properties of Precipitated Cobalt Ferrite Nanoparticles. *Journal of Molecular Structure*. 1140: 32-38. <http://dx.doi.org/10.1016/j.molstruc.2016.09.067>.
- [9] Sha, A. L., Hassan R.A, Alharbi, A. A., Alomayri, T. and Alamri, H. 2017. Magnetic Hyperthermia using Cobalt Ferrite Nanoparticles: The Influence of Particle Size. *Int J Adv Technol*. 8: 196. <https://doi.org/10.4172/0976-4860.1000196>.
- [10] Ponce, A. S., Chagas, E. F., Prado, R. J., Fernandes, C. H. M., Terezo, A. J., Baggio-Saitovitch, E. 2013. High Coercivity Induced by Mechanical Milling in Cobalt Ferrite Powders. *Journal of Magnetism and Magnetic Materials*. 344: 182-187. <https://doi.org/10.1016/j.jmmm.2013.05.056>.
- [11] de Freitas, M. R., de Gouveia, G. L., Costa, L. J. D., de Oliveira, A. J. A., Kiminami, R. H. G. A. 2016. Microwave Assisted Combustion Synthesis and Characterization of Nanocrystalline Nickel-doped Cobalt Ferrites. *Materials Research*. 19(Suppl. 1): 27-32. <http://dx.doi.org/10.1590/1980-5373-MR-2016-0077>.
- [12] Xavier S, M. K. Jiji, Smitha Thankachan, E. M. Mohammed. 2014. Effect of Sintering Temperature on the Structural and Electrical Properties of Cobalt Ferrite Nanoparticles. *AIP Conference Proceedings*. 1576: 98. <https://doi.org/10.1063/1.4861992>.
- [13] Toby, B. H. 2001. EXPGUI, A Graphical User Interface for GSAS. *Journal of Applied Crystallography*. 34: 210. <https://doi.org/10.1107/S0021889801002242>.
- [14] Imam, N. G., Ismail, S. M., Elbahrawy, M. Y. and Hashhash A. M. 2014. Photoluminescence, Magnetic and Electrical Properties of Co-ferrite Nanoparticles Synthesized via Sol-gel Auto-combustion Method. *Int. J. Nanoparticles*. 7(3/4): 170-189. <https://doi.org/10.1504/ijnp.2014.067601>.
- [15] Nagasa, B. D., Raghavender A. T., Kabeta, K. L., Anjaneyulu, T., Regasa, M. B. 2015. Size Induced Structural and Magnetic Properties of Nanostructured Cobalt Ferrites Synthesized by Co-precipitation Technique. *Sci. Technol. Arts Res*. 4(1): 84-87. <http://dx.doi.org/10.4314/star.v4i1.13>.
- [16] Kadhum, J. K. and Zeyad, T. I. 2014. Microwave Properties of Spinel Ferrite. *International Journal of Application or Innovation in Engineering & Management (IJAIEM)*. 3(9): 93-97. https://ijaiem.org/pabstract_Share.php?pid=IJAIEM-2014-09-03-1.
- [17] Yana Taryana, Yuyu Wahyu, Azwar Manaf, M. Manawan, Wisnu Ari Adi. 2022. Structural and Microwave Absorption Properties of $\text{BaFe}(12-2x)\text{SnxZnxO}19$ ($x=0.05-1.0$) Ceramic Magnets. *Materialia*. 23(2022): 101455. <https://doi.org/10.1016/j.mtla.2022.101455>.
- [18] Marki Microwave. 2017. Return Loss to VSWR Conversion Table, 215 Vineyard Court, Morgan Hill, CA 95037. www.markimicrowave.com.
- [19] Huang, X., Zhang, J., Xiao, S. and Chen, G. 2014. The Cobalt Zinc Spinel Ferrite Nanofiber: Lightweight and Efficient Microwave Absorber. *J. Am. Ceram. Soc.* 97(5): 1363-1366. <https://doi.org/10.1111/jace.12909>.
- [20] Li, G. M., Wang, L. C. and Xu, Y. 2014. Templated Synthesis of Highly Ordered Mesoporous Cobalt Ferrite and Its Microwave Absorption Properties. *Chin. Phys. B*. 23(8): 088105. <https://doi.org/10.1088/1674-1056/23/8/088105>.
- [21] Ismail, M. M., Rafeeq, S. N., Sulaiman, J. M. A., Mandal, A. 2018. Electromagnetic Interference Shielding and Microwave Absorption Properties of Cobalt Ferrite CoFe_2O_4 /polyaniline Composite. *Applied Physics A*. 124(380): (1-12). <https://doi.org/10.1007/s00339-018-1808-x>.